2. V. Ya. Shkadov, "Some methods and problems of hydrodynamic stability theory," Tr. Mosk. Gos. Univ., No. 25 (1973).
3. A. S. Lyshevskii, Principles of Liquid Fractionation by Mechanical Pressure Atomizers [in Russian], Novocherkassk. Politekh. Inst., Novocherkassk (1961).
4. Yu. F. Dityakin, L. A. Klyachko, B. V. Novikov, and V. I. Yagodkin, Liquid Atomization [in Russian], Mashinostroenie, Moscow (1977).
5. Yu. S. Kachanov, V. V. Kozlov, and V. Ya. Levchenko, Development of Turbulence in a Boundary Layer [in Russian], Nauka, Novosibirsk (1982).
6. V. I. Eliseev, "Stability of a jet of ideal nonweightless liquid," Zh. Prikl. Mekh. Tekh. Fiz., No. 3 (1981).
7. N. Friedenraich, "Flow of a liquid film over a rotating disk," Rev. Mex. Fisica, 25, No. 2 (1976).
8. L. A. Dorfman, "Flow and heat exchange in a viscous liquid layer on a rotating disk," Inzh.-Fiz. Zh., 12, No. 3 (1967).
9. G. I. Lepekhin, G. V. Ryabchuk, et al., "Viscous liquid flow on a rotating plane disk," Teor. Osn. Khim. Tekhnol., 15, No. 3 (1981).
10. A. F. Charwat and R. E. Kelly, "The flow and stability of thin liquid films on a rotating disk," J. Fluid Mech., 53, No. 2 (1972).
11. H. Espig and R. Hoyle, "Waves in a thin liquid layer on a rotating disk," J. Fluid Mech., 22, No. 4 (1965).
12. A. I. Butuzov and I. I. Pukhovoi, "Flow regimes of a liquid film on a rotating surface," Inzh.-Fiz. Zh., 31, No. 2 (1976).

SPATIAL DISTORTION OF MEAN BOUNDARY LAYER BY NATURAL OSCILLATIONS

N. A. Zheltukhin and N. M. Terekhova

UDC 532.526

1. One of the stages in the nonlinear growth of disturbances in the transition region of an incompressible boundary layer on a flat plate is the generation and subsequent growth of three-dimensional oscillating field as a result of which disturbances are found to have clearly defined spatial structure with alternating maxima (crests or peaks) and minima (valleys) of amplitudes in the transverse direction (along z axis). Reasons for the appearance of such natural wave structure have not yet been explained conclusively. One of them could be the interaction of the initial finite amplitude plane disturbances with small, local, spatial nonuniformities in the mean flow, which leads to the generation of a pair of oblique Tollmien–Schlichting waves [1]. Natural weak disturbances in the leading edge region can also be the source of subsequent real wave fields.

Subsequent triple-wave resonant interaction in the nonlinear growth region of plane waves lead to the amplification of three-dimensional components [2, 3]. Thus, it was shown in [4] that on attaining the threshold amplitudes $\varkappa_d \sim 0.007$ there is a strong growth of oblique waves so that the characteristic disturbance field of the boundary layer takes the form of an additive field of Tollmien–Schlichting waves:

$$\begin{aligned} u'(x, y, z, t) &= \varkappa_d u_d(y)\, e^{\Omega_1} + 2\varkappa_T u_T(y)\, e^{\Omega_2} \cos \beta z, \\ v'(x, y, z, t) &= \varkappa_d v_d(y)\, e^{\Omega_1} + 2\varkappa_T v_T(y)\, e^{\Omega_2} \cos \beta z, \\ w'(x, y, z, t) &= 2\varkappa_T i w_T(y)\, e^{\Omega_2} \sin \beta z, \end{aligned} \tag{1.1}$$

where $\Omega_1 = i\alpha_1(x - C_1 t)$, $\Omega_2 = i\alpha_2(x - C_2 t)$. The inclination of oblique waves to the plane flow is determined as $\theta = \arctan \beta/\alpha$. The presence of such characteristic disturbances leads to a qualitative change in the structure of the mean flow, viz., minimum values of mean velocity at crests and maximum values at valleys are observed. This is interpreted as the appearance of a system of localized streamwise vortices in the boundary layer which are periodic

Novosibirsk. Translated from Zhurnal Prikladnoi Mekhaniki i Tekhnicheskoi Fiziki, No. 6, pp. 117–122, November–December, 1983. Original article submitted October 25, 1982.

0021-8944/83/2406-0871$07.50

along the z axis and stationary (or quasistationary) in time (Benny–Lin vortices). A study of secondary vortex fields has been carried out in a number of papers [5-7] using weak nonlinear theory. It is shown that the presence of weak three-dimensionality $\varkappa_d >> \varkappa_t$ activates weak horseshoe vortex occupying the position determined by the half-period of the waves (1.1) $0 \leq \beta z \leq \pi$. An increase in the growth parameter $\varkappa_t$ makes this secondary structure complex, and when $\varkappa_t >> \varkappa_d$ the vortex structure is described by a system of counter-rotating vortex pairs. Such a limiting case is considered in [8] on the basis of a numerical solution of Reynolds equation for the mean flow which made it possible not only to establish the quantitative dependence of vortex formation on $\varkappa_t$ but also to compute streamwise components of mean velocities that was not done in the above-referenced studies.

The present study, which has been carried out for waves of the type (1.1), extends and defines the application of the model based on the Reynolds equation to describe complex secondary flows during transition.

2. Thus, in the flat plate boundary layer on which the mean flow is described by the equation

$$\Phi_{\eta\eta\eta} + \Phi\Phi_{\eta\eta} = 0,\ \eta = y(\bar{U}_0/2\nu x)^{1/2},\ U_0 = \Phi_\eta, \qquad (2.1)$$
$$\Phi = \Phi_\eta = 0(\eta = 0),\quad \Phi_\eta \to 1\ (\eta \to \infty),$$

natural oscillations (1.1) appear in the region of the nonlinear growth of disturbances. Amplitude functions of the waves u, v, and w satisfy the linearized Navier–Stokes equations [9]. In order to simplify the analysis, we assume that the phases of Ω_1 and Ω_2 are equal or, as shown in [7], the introduction of frequency disparity in waves of different scales that results in a 10-15% difference in phase velocities C_1 and C_2 is not significant. However, we note that such a difference can be introduced through the phase difference $\Delta\Omega$, which will be present in equations as a coefficient.

The secondary flow induced in (1.1) takes the form of spatial flow $U = U(\eta, z)$, $V = V(\eta, z)$, and $W = W(\eta, z)$ and is described by the system

$$VU_\eta + WU_z - (1/\mathrm{Re})(U_{\eta\eta} + U_{zz}) = -f_1; \qquad (2.2a)$$

$$VV_\eta + WV_z + P_\eta - \frac{1}{\mathrm{Re}}(V_{\eta\eta} + V_{zz}) = -\frac{\partial\langle v'^2\rangle}{\partial\eta} - \frac{\partial\langle v'w'\rangle}{\partial z}, \qquad (2.2b)$$

$$VW_\eta + WW_z + P_z - \frac{1}{\mathrm{Re}}(W_{\eta\eta} + W_{zz}) = -\frac{\partial\langle v'w'\rangle}{\partial\eta} - \frac{\partial\langle w'^2\rangle}{\partial z},$$
$$V_\eta + W_z = 0.$$

The right-hand sides contain Reynolds stresses obtained statistically by averaging respective second moments whose form is concretized below. The similarity parameter is the transverse coordinate and the equations themselves are nondimensionalized with respect to the reference velocity $\bar{U}_0$ and the boundary layer thickness $\bar{\delta}$.

According to [10], the zone of spatial growth of disturbance and the establishment of associated secondary flows are on the order of $\bar{\delta}$. The present study looks at the region beyond this zone. The closure of (2.2) is carried out within the framework of monoharmonic approximation [3], i.e., for the fundamental harmonic of the type (1.1).

System (2.2) can be split and it is possible to find streamwise vortices with components V and W independently from the curve $U(\eta, z)$. As shown in [8], it is completely justified to neglect convective terms in (2.2b) for the amplitude $\varkappa_t \leq 0.01$ ($\theta \sim \pi/6$) which makes it possible to bring Eq. (2.2b) for the stream function $V = \psi_z$ and $W = -\psi_\eta$ to the form

$$\frac{1}{\mathrm{Re}}\left(\frac{\partial^2}{\partial\eta^2} + \frac{\partial^2}{\partial z^2}\right)^2\psi + F(\eta, z) = 0. \qquad (2.3)$$

The total moment of forces due to Reynolds stresses $F(\eta, z)$ is made up of the generative action of three-dimensional waves F_t and the moment F_{dt} caused by the nonlinear coupling of two- and three-dimensional waves, and for (1.1) it is written in the form

$$F(\eta, z) = \varkappa_T^2\mathcal{F}_T(\eta)\sin 2\beta z + \varkappa_T\varkappa_d\mathcal{F}_{dT}(\eta)\sin\beta z,$$

where

$$\mathcal{F}_T(\eta) = \langle v_T w_T\rangle_{\eta\eta} + 2\beta\left(\langle v_T^2\rangle_\eta + \langle w_T^2\rangle_\eta + 2\beta\langle v_T w_T\rangle\right), \qquad (2.4)$$

$$\mathcal{F}_{d,T}(\eta) = \langle v_d w_T \rangle_{\eta\eta} + \beta(\langle v_d v_T \rangle_\eta + \beta \langle v_d w_T \rangle).$$

Here the amplitude functions are given within angular brackets and are rewritten in the following manner

$$\langle vw \rangle = v_i w_r - v_r w_i, \quad \langle v^2 \rangle = v_r^2 + v_i^2, \quad \langle w^2 \rangle = w_r^2 + w_i^2.$$

Since (2.3) is linear, its solution is written in the form

$$\psi(\eta, z) = \Psi_T(\eta) \sin 2\beta z + \Psi_{dT}(\eta) \sin \beta z,$$

and the amplitude functions satisfy the following equations

$$\begin{aligned} (D^2 - 4\beta^2)^2 \Psi_T &= -\varkappa_T^2 \operatorname{Re} \mathcal{F}_T(\eta), \\ (D^2 - \beta^2)^2 \Psi_{dT} &= -\varkappa_T \varkappa_d \operatorname{Re} \mathcal{F}_{d,T}(\eta). \end{aligned} \tag{2.5}$$

The boundary-value problem for (2.5) is determined from physical conditions

$$V = W = 0 \text{ for } \eta = 0 \text{ and } V, W \to 0 \text{ for } \eta \to \infty.$$

The first two conditions make it possible to determine

$$\Psi_T = \Psi_{d,T} = D\Psi_T = D\Psi_{d,T} = 0 \text{ for } \eta = 0, \tag{2.6a}$$

and the two second conditions are replaced by asymptotic relations which, for large η, can be written in the form

$$L_1 \Psi_T = L_2 \Psi_{d,T} = DL_1 \Psi_T = DL_2 \Psi_{dT} = 0. \tag{2.6b}$$

Here $L_1 = D^2 + 4\beta(D + \beta)$, $L_2 = D^2 + \beta(2D + \beta)$. The upper boundary $\eta = Y$, as a rule, corresponded to $(1.5\text{-}2)\delta_{1am}$. Equations (2.5) and (2.6) determine the vortex components of the secondary flow $V(\eta, z) = 2\beta\Psi_T \cos 2\beta z + \beta\psi_{dT} \cos \beta z$, $W(\eta, z) = -\Psi'_T \sin 2\beta z - \Psi'_{dT} \sin \beta z$. The period of spatial repetitions should be chosen so that $T = 2\pi/\beta$. The streamwise component $U(\eta, z)$ is determined in the region $[0 \leq \eta \leq Y, 0 \leq z \leq T]$ from (2.2a) and boundary conditions

$$U(0, z) = U_\eta(Y, z) = 0, \{U, U_z\}(\eta, 0) = \{U, U_z\}(\eta, T).$$

The right-hand side of f_1 makes it possible to decouple the following active wave components of (1.1):

three-dimensional distortion of U by three-dimensional waves

$$f_{1T} = \varkappa_T^2 (\langle u_T v_T \rangle_\eta + 2\beta \langle u_T w_T \rangle) \cos 2\beta z,$$

three-dimensional distortion due to wave interaction

$$f_{1dT} = \varkappa_T \varkappa_d (\langle u_d v_T \rangle_\eta + \langle u_T v_d \rangle_\eta + \beta \langle u_d w_T \rangle) \cos \beta z,$$

two-dimensional distortion due to two- and three-dimensional waves $f_{1d} = \kappa^2_T \langle u_T v_T \rangle_\eta + \kappa^2_d \langle u_d v_d \rangle_\eta / 2$. Here, $\langle uv \rangle = u_r v_r + u_i v_i$, $\langle uw \rangle = u_i w_r - u_r w_i$. In the absence of disturbances, (2.2a) determines laminar distribution of U_0 if forces $f_{10} = -\Phi_{\eta\eta\eta}/\mathrm{Re}$ are introduced on the right-hand side. Thus, finally, $f_1 = f_{1T} + f_{1d} + f_{1dT} + f_{10}$.

3. The realization of the above problem can be illustrated by modeling secondary flows arising in the regions close to critical Reynolds number based on linear theory. As shown in studies on the nature of bifurcation of Navier–Stokes equations [3, 11], the nonlinear growth of waves in this region only marginally alters Re_*, so that the choice of waves with eigenvalues corresponding to neutral disturbances in this region is justified.

Figure 1 shows amplitude functions of generating forces $\mathcal{F}(\eta)$ along with the quantities $\langle uv \rangle_\eta$ and $\langle uw \rangle$, from which it is possible to get the components of f_1 (solid lines represent three-dimensional waves and dashed lines indicate two- and three-dimensional waves). The given data correspond to $\theta \sim 25°$. The shape of the curve agrees quite well, very insignificantly differing at the maxima. With an increase in θ, the difference in the distributions increases. A typical shape of amplitude functions of the vortex (2.5) is shown in Fig. 2 for the same θ and $\varkappa_d = \varkappa_t = 0.02$. It appeared that, all other conditions being the same, the strength of the vortex induced by three-dimensional waves is approximately 5 times more than that determined by forces $\mathcal{F}_{dT}$. Similar relations are also observed for other param-

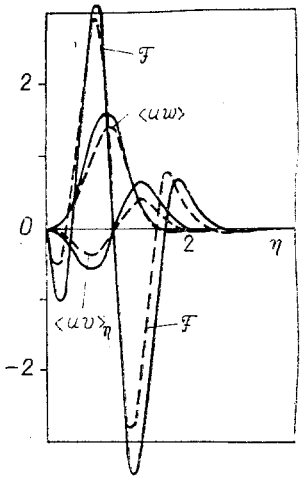

Fig. 1

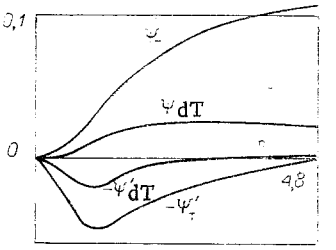

Fig. 2

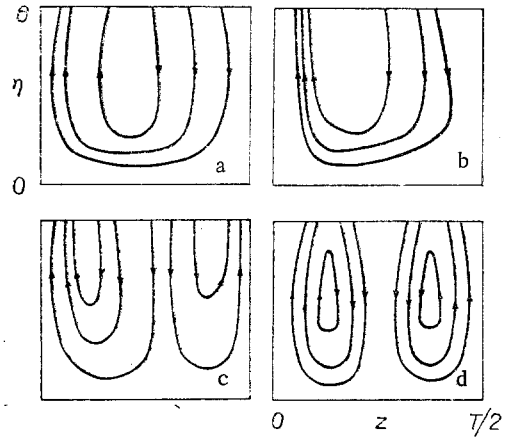

Fig. 3

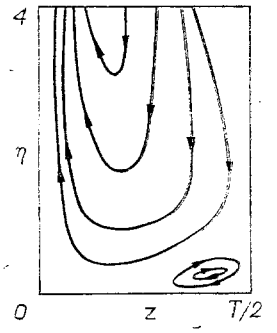

Fig. 4

eters κ_d and κ_t. Vortex structures for certain interesting ratios of κ_d and κ_t are shown in Fig. 3. When the plane wave dominates in the flow ($\kappa_d/\kappa_t = 20$, Fig. 3a), a very weak vortex [$\psi_{max}(z \sim T/4) = 0.001$] occupies the position $0 \leq z \leq T/2$, quite symmetrically distributed in the flow field. The growth in amplitude of three-dimensional waves ($\kappa_d/\kappa_t = 10$, Fig. 3b) destroys the symmetry in distribution (stream function ψ = const are concentrated in regions of small z) and increases $\psi_{max}(z \sim T/6) = 0.003$. In regions $\kappa_d \sim \kappa_t$ (Fig. 3c), the vortex structure becomes complex, being enriched by weaker counter-rotating vortex which forces out the first from the regions $T/3 \leq z \leq T/2$. The strength of the initial vortex in this case is a maximum $\psi_{max}(z \sim T/8) = 0.125$, and for the additional vortex $\psi_{max}(z \sim 3T/8) = 0.09$. The domination of oblique waves $\kappa_t \gg \kappa_d$ (Fig. 3d) leads to diagrams shown in [8], i.e., to symmetrically located and distributed pair dividing in $z = T/4$ with $\psi_{max}(z = T/8) \sim 0.1$.

According to experiments [12], a change in sign of the total transverse velocity was observed very close to the wall under certain flow conditions. This change in W was interpreted as the appearance of weak wall vortices, lying below the critical layer, which are subjected to the influence of the wall. For Re_* and $\theta \sim 25°$, such a situation exists when $\kappa_d = 0.05$ in the range $10 \leq \kappa_d/\kappa_t \leq 25$ (Fig. 4). An increase in θ at fixed Re leads to a decrease in the limiting amplitude κ_d for which this condition is possible, but the necessary condition for the appearance of the complex structures is the dominant presence of plane waves that is expressed in the conservation of the range of $\kappa_d\kappa_t$ of its existence. For the lower branch of the neutral curve at $Re \sim 10^3$ such a condition is met by the values $\kappa_d = 0.01$, $\theta \sim 50°$, and $7 \leq \kappa_d/\kappa_t \leq 11$.

Such a detailed analysis of vortex structures helps in supplementing [7] by quantitative relations and shows that within the framework of linear theory, descriptions of the phenomena

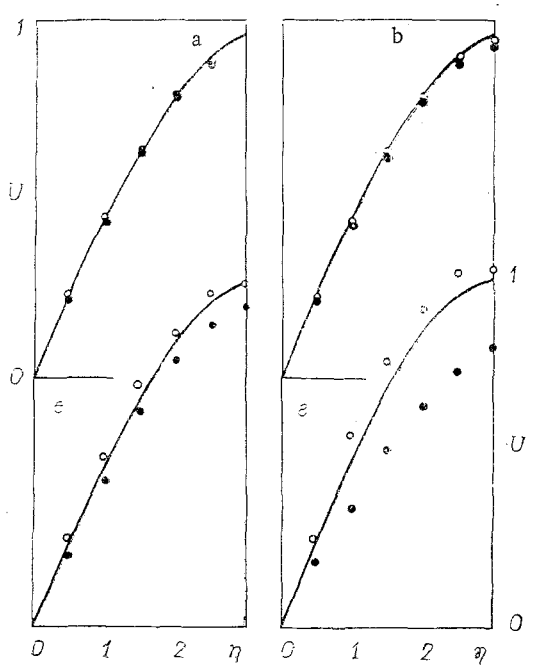

Fig. 5

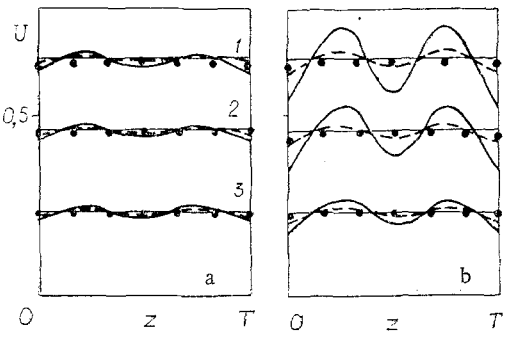

Fig. 6

either from the position of mean flows or from the position of perturbation technique with weak nonlinear theory are completely identical and topologically agree with experimentally observed thin layer of secondary flow.

It appeared that the presence of coherent structures in the boundary layer in the form of longitudinal vortices causes the following redistribution of mass and momentum: at certain spatial locations vortices entrain low-speed wall layer, carry it to the outer flow region, which is accompanied by a decrease in fullness of local distributions $U(\eta, z)$. In other regions an opposite phenomenon occurs, viz., vortices bring fluid from the potential core of the flow as a result of which the fullness of near-wall layers increases. Such a redistribution, obtained within the framework of (2.2a), is shown in Fig. 5 for $\kappa_d = 0.005$, $\kappa_d/\kappa_t = 10$, 5, 1, and 0.5 (a-d, respectively). Here the solid lines indicate laminar flow $U_0 = \Phi_\eta$, and the points indicate computed values of the maxima and minima of the curves $U(\eta, z)$.

The resulting picture of distortion in U is shown in Fig. 6 for $\theta \sim 25°$ and $\kappa_d/\kappa_t = 2$, 4, and 10 (solid and dashed lines and points). Figure 6a is for $\kappa_d = 0.0025$ and Fig. 6b is for $\kappa_d = 0.005$. Solid, horizontal lines 1-3 represent laminar flow U_0 for $\eta = 1.5$, 1, and 0.5, respectively. From this it is possible to obtain curves $U(\eta, z)$ for any section $z = \text{const}$. For certain values of the parameter κ_t in sections $z = 0$, profiles $U(\eta, 0)$ have inflection points which could be the cause for the local growth of disturbances at these spatial locations. However, in the outer flow region it is not always possible to attain the undisturbed external flow velocity for the longitudinal profile U. This reflects the inadequacy of the monoharmonic approximation in these regions.

It is necessary to mention a few words on the growth time for the above phenomena. Since system (2.2) describes stationary or quasistationary flows, the method used in [13] to solve (2.2a) makes it possible to estimate the slow time t_1 and compare it with the rapid time $t = 2\pi/\alpha C$ of the wave process (1.1). It appeared that in order to establish the distributions shown in Fig. 5, the flow should be subject to about 5 periods of rapid time. This relation decreases with increase in the angle θ and wave amplitude κ_t. Estimates for V and W are somewhat worse and here t_1/t is estimated to a few tens.

LITERATURE CITED

1. I. Tani, "Some thoughts on boundary-layer transition," in: Laminar-Turbulent Transition: Symp., Stuttgart (1979); Berlin e.a. (1980).
2. A. D. D. Craik, "Nonlinear resonant instability in boundary layers," J. Fluid Mech., 50, Pt. 2 (1971).

3. M. A. Gol'dshtik and V. N. Shtern, Hydrodynamic Stability and Turbulence [in Russian], Nauka, Novosibirsk (1977).
4. C. Nakaya, "Three-dimensional waves in boundary layer," in: Laminar-Turbulent Transition: Symp., Stuttgart (1979); Berlin e.a. (1980).
5. D. J. Benny and C. C. Lin, "On the secondary motion induced by oscillations in a shear flow," Phys. Fluids, 3, No. 4 (1960).
6. D. J. Benny, "Finite amplitude effects in an unstable laminar boundary layer," Phys. Fluids, 7, No. 3 (1964).
7. B. N. Antar and F. G. Collins, "Numerical calculation of finite amplitude effects in unstable laminar boundary layers," Phys. Fluids, 18, No. 3 (1975).
8. N. A. Zheltukhin and N. M. Terekhova, "Secondary flows in unstable boundary layers," Zh. Prikl. Mekh. Tekh. Fiz., No. 4 (1981).
9. R. Betchov and W. O. Criminale, Jr., Stability of Parallel Flows, Academic Press (1967).
10. V. N. Zhigulev, "Nonlinear theory of disturbance growth," in: Aerodynamics and Physical Kinetics [in Russian], Inst. Theoretical and Applied Mechanics, Siberian Branch, Academy of Sciences of the USSR, Novosibirsk (1977).
11. S. A. Gaponov and B. Yu. Skobelev, "Secondary similarity conditions for Blasius flow," in: Problems in Hydrodynamics [in Russian], Institute of Theoretical and Applied Mechanics, Siberian Branch, Academy of Sciences of the USSR, Novosibirsk (1975).
12. P. S. Klebanoff, K. D. Tidstrom, and L. M. Sargent, "The three-dimensional nature of boundary-layer instability," J. Fluid Mech., 12, Pt. 1 (1962).
13. N. N. Yanenko, The Method of Fractional Steps in the Solution of Multivariable Problems in Mathematical Physics [in Russian], Nauka, Novosibirsk (1967).

THERMAL CONVECTION IN A HORIZONTAL LAYER WITH LATERAL HEATING

A. G. Kurdyashkin, V. I. Polezhaev, and A. I. Fedyushkin

UDC 536.252+532.5+532.68

1. Introduction. We consider convection in a horizontal layer in a uniform gravitational field with a thermal gradient directed along the layer. Along with the well-known Rayleigh—Benard problem on the convection in a layer heated from below, this one of the fundamental problems in the theory of thermal convection. Recently, there has been interest in this problem because of new experimental techniques, and various engineering and geophysical applications (transport processes during crystallization, in solar collectors, in shallow reservoirs, etc.). Because the state of hydrostatic equilibrium does not exist, unlike the case of heating from below, here convection is induced for any nonzero horizontal temperature difference. However, the intensity of convection and its effect on the temperature (or concentration) field depends significantly on the length-to-width ratio of the layer, and the Rayleigh and Prandtl numbers. An essential role is played by the heat-exchange conditions at the upper and lower horizontal surfaces; these conditions vary widely in practice. Thus, there are a large number of different multiparameter convective processes whose study requires a mathematical model based on the Navier—Stokes equations, and a test of the adequacy of the model by comparison with experiment.

The case most studied theoretically is the situation where identical (linear) temperature distributions are given along both horizontal boundaries. Several papers have considered the flow stability in this case for an infinitely long layer [1, 2]. Convection leads to an unstable vertical temperature distribution at the lower and upper boundaries of the layer.

In the present paper, we experimentally and theoretically study another case, where the horizontal boundaries of the layer are thermally insulated, and different temperatures are specified on the lateral walls. Then convection always leads to an unstable vertical temperature distribution, and this essentially changes the flow structure and heat transport. A

Translated from Zhurnal Prikladnoi Mekhaniki i Tekhnicheskoi Fiziki, No. 6, pp. 122-128, November-December, 1983. Original article submitted October 10, 1982.

 0021-8944/83/2406-0876$07.50